Paleogeographic differences in temperature, water depth and conodont biofacies during the Late Devonian

Catherine Girard, Jean-Jacques Cornee, Michael Joachimski, Anne-Lise Charruault, Anne-Béatrice Dufour, Sabrina Renaud

▶ **To cite this version:**

HAL Id: hal-01895836

https://hal.umontpellier.fr/hal-01895836

Submitted on 3 Jun 2022

1   **Paleogeographic differences in temperature, water depth and conodont biofacies**

2   **during the Late Devonian**

3

4   Girard, Catherine[1, *], Cornée, Jean-Jacques[2, 3], Joachimski, Michael M.[4], Charruault, Anne-

5   Lise[1], Dufour, Anne-Béatrice[5], Renaud, Sabrina[5]

6

7   [1] Institut des Sciences de l'Evolution, Université de Montpellier, UMR5554 CNRS, IRD,

8   EPHE, Place Eugène Bataillon, CC65, 34095 Montpellier cedex, France

9   (catherine.girard@umontpellier.fr; anne-lise.charruault@umontpellier.fr)

10   [2] Géosciences Montpellier, Université de Montpellier, 34095 Montpellier Cedex 05,

11   France (jean-jacques.cornee@gm.univ-montp2.fr)

12   [3] current address : Université des Antilles, Campus de Fouillole, 97170 Pointe-à-Pitre,

13   France

14   [4] GeoZentrum Nordbayern, University of Erlangen-Nuremberg, Schlossgarten 5, D-

15   91054 Erlangen, Germany (michael.joachimski@fau.de)

16   [5] Laboratoire de Biométrie et Biologie Evolutive, UMR 5558, Université de Lyon,

17   Université Lyon 1, CNRS, 69100 Villeurbanne, France (sabrina.renaud@univ-lyon1.fr;

18   anne-beatrice.dufour@univ-lyon1.fr)

19

20   *corresponding author

21

22   **Abstract**

23

24   The Famennian (Late Devonian) started after and ended with two of the seven largest

25   crises of the Phanerozoic, the Kellwasser and Hangenberg events, respectively. In

26   between, global environmental trends have been identified, involving cooling and

27   eustatic regression. Tropical and subtropical marine faunas were largely cosmopolitan.

28   Overall, this suggests that the Famennian was marked by long-term environmental

29   changes occurring in a relatively homogeneous manner despite being punctuated by

30   several short-term events of limited faunal impact. How these trends were modulated

31   according to geographic location is investigated in this study by comparing two

32   continuous outcrops in the Montagne Noire (Col des Tribes section, France) and in Saxo-

33   Thuringia (Buschteich section, Germany). Both were located in the subtropical area

34   during this period and belonged to two former microcontinents bracketed between the

35   closing Rheic Ocean and Gondwana. Sedimentary facies, oxygen isotopes, and the

36   generic conodont composition (biofacies) were studied in a high resolution and in the

37   same rock samples. Sedimentary facies provided an estimate of water depth and oxygen

isotopes were used as paleotemperature proxy. Conodont biofacies were analyzed using a principal component analysis, allowing the expression of the variations in the two outcrops on the same axes, and a quantitative comparison with the other proxies. Sea-level and temperature variations were different between the two areas. Saxo-Thuringia displayed stable deep and warm conditions throughout. In contrast, the environment of the Montagne Noire was shallower and cooler during the Late and latest Famennian compared to the Early and Middle Famennian, congruent with the global change evidenced elsewhere. The location of Saxo-Thuringia, close to the first point of closure of the Rheic Ocean, might have favored active tectonics, causing a local departure from the eustatic trend. The stable temperatures at BU during the Late and latest Famennian may be due to the position of Saxo-Thuringia in the remnant Rheic Ocean, limiting water mass exchange with open seas, and favoring the persistence of warm conditions. Offshore taxa persisted later at high abundance in the Saxo-Thuringian record. The two conodont biofacies records were otherwise very comparable. This suggests that other factors mitigated the water depth forcing on these conodont assemblages.

1. Introduction

The Famennian is well known for being bracketed by two of the most important biological crises in the Earth's history: the Upper Kellwasser Event just before the Frasnian-Famennian boundary (e.g. McGhee, 1996; Schindler, 1993; Walliser, 1996) and the Hangenberg Crisis punctuating the Devonian-Carboniferous boundary (e.g. Becker et al. 2016; Kaiser et al. 2008, 2015; Walliser, 1996). Many studies were devoted to these crises, allowing a fine-scale characterization of the biotic and abiotic variations during the hundred thousand years involved in these worldwide perturbations (Becker et al., 2012; Corradini, 2003; Girard and Feist, 1997; Joachimski et al., 2009; McGhee, 1996; Sandberg et al., 1988; Walliser, 1996). Environmental changes also occurred during the time interval between the crises (ca. 13 Myr, Becker et al., 2012), but deserved much

71   less attention. Short-term events have nevertheless been described, with minor impact

72   on the faunas (e.g. *Annulata* Events by House, 1985; Korn, 2004; Hartenfels, 2011;

73   Hartenfels and Becker, 2017; Dasberg Crisis by Becker, 1993; Hartenfels and Becker,

74   2009; Hartenfels, 2011; Condroz Events by Becker, 1993; Becker and House, 1997). A

75   regressive trend punctuated by minor transgressive-regressive couplets has been

76   evidenced for the Famennian (Johnson et al., 1985, 1996). Global cooling inferred from

77   oxygen isotope data has been suggested for the same interval (Joachimski et al., 2004,

78   2009), an interpretation supported by independent evidence of Latest Famennian

79   glacial deposits described from South America (Caputo et al., 2008; Isaacson et al.,

80   2008). The congruence of climate cooling and a regressive trend is therefore coherent in

81   this eustatic context. Tropical and subtropical marine faunas were cosmopolitan at the

82   generic level (Feist and Becker, 1997; Korn and De Baets, 2015; Mottequin et al., 2013;

83   Spalletta et al., 2017) suggesting rather homogeneous environmental conditions and

84   efficient exchanges between the faunas. Conodonts, small, nektonic animals of chordate

85   affinities, were an abundant part of this marine fauna. Their taxonomic identification

86   provides a detailed stratigraphic framework for this period (Hartenfels, 2011; Spalletta

87   et al., 2017; Ziegler, 1962; Ziegler and Sandberg, 1984; 1990). Conodonts can also give

88   paleoenvironmental indications because conodont genera distribution was influenced

89   by several factors (Lüddecke et al., 2017), notably water depth (Sandberg, 1976; Seddon

90   and Sweet, 1971). The congruence of temporal variations in the conodont biofacies (i.e.

91   assemblage composition of the different genera) in different sections supported that the

92   Famennian was marked by long-term environmental changes that were not durably

93   perturbed by the short-term events punctuating it (Corradini, 2003; Girard et al., 2014;

94   2017).

95   This view, however, can also be the consequence of the paucity of detailed

96   records in different paleogeographic areas. Famennian paleogeography was

97   characterized by the closure of the Rheic Ocean bracketing microcontinents derived

98   from Gondwana (e.g. Franke et al., 2017; Stampfli et al., 2013) (Fig. 1). Discrepancies in

99   relative sea-level changes have been reported from these microcontinents (e.g. in the

100   Saxo-Thuringian area) and attributed to tectonic movements overprinting the global

101   eustatic trend (Girard et al., 2017). This raises the question whether the environmental

102   trends evidenced so far are of global significance, and/or whether local/regional factors

103 related to tectonics and paleogeographic changes interfered with these (presumed)

104 global trends.

105 To address these questions, we studied two recently described sections having a

106 detailed record from the Late Frasnian to the end-Famennian (Girard et al., 2014, 2017).

107 The Col des Tribes (CT) section in the Montagne Noire was part of the Armorica

108 microcontinent, whereas the Buschteich section (BU) was located on the Saxo-

109 Thuringian microplate. Hence, both sections were located on former microcontinents

110 bracketed between the closing Rheic Ocean and Gondwana (Fig. 1). Water depth and

111 approximate position relative to the shore were assessed based on the macroscopic

112 description of the sediments as well as microfacies analysis (e. g. Flügel, 2004). Despite

113 limitations due to the scarcity of preserved bioclasts in the sediments (e.g. Brett and

114 Allison, 1998), this approach provided a paleoenvironmental estimate directly based on

115 the depositional environment. Water depths derived from sedimentological analysis

116 were compared with conodont biofacies, which have been proposed to react more

117 sensitive to water-depth changes than microfacies (Lüddecke et al., 2017). Nevertheless,

118 as for any biotic record, evolutionary changes through time (changes in water depth

119 preferences, decrease or increase in response to biotic factors such as predation or

120 competition) may interfere with the paleoenvironmental signature (Belka and Wendt,

121 1992). A multivariate approach was developed to quantitatively compare the conodont

122 assemblages in the studied sections. In addition, paleotemperatures were reconstructed

123 using oxygen isotopes measured on conodont apatite.

124 A strength of this study is that the three proxies are derived from the same rock

125 samples taken at a comparable temporal resolution, allowing for detailed and

126 quantitative comparisons. The following questions are addressed: (1) Did

127 environmental changes affect similarly and at the same pace both areas, and if not, how

128 to interpret any discrepancies? (2) Did water depth and temperature covary, as

129 expected for eustatic trends during a global cooling culminating with the Devonian-

130 Carboniferous boundary glaciation (Buggisch et al. 2008; Caputo et al., 2008; Isaacson et

131 al., 2008)? (3) Was the forcing of water depth changes recorded as expected on

132 conodont biofacies? In that context, did conodont biofacies rather react to local

133 deviations from, or to globally recorded paleoenvironmental trends?

134

135 **2. Geological setting**

136   During the Late Devonian, the Col des Tribes (CT; Montagne Noire/France; Girard

137   et al., 2014) and Buschteich (BU; Thuringia/Germany; Girard et al., 2017) sections were

138   located in subtropical latitudes on different microcontinents (Fig. 1). These

139   microcontinents progressively migrated towards the equator and Laurussia during this

140   period due to the closure of the Rheic Ocean (Franke et al., 2017). The absence of

141   provincialism in benthic faunas compared to Laurussian faunas suggests that the Rheic

142   Ocean was, at that time, already reduced (Feist and Becker, 1997; Mottequin et al.,

143   2013). It has been proposed that the Saxo-Thuringia microcontinent, on which BU was

144   located, was situated in the middle of the sea between the remnant Rheic Ocean and the

145   Paleotethys (Franke et al., 2017) during the Late Frasnian (375 Ma). By the latest

146   Famennian (~360 Ma), this seaway was almost or completely closed, locating BU at the

147   margin of the remnant Rheic Ocean (Fig. 1). The Montagne Noire, including CT, was

148   located on the Armorica microcontinent which was presumably positioned further

149   towards the Paleotethys Ocean. Nevertheless, the precise location of these

150   microcontinents relative to Laurussia as well as their position relative to each other is

151   debated (e.g. Eckelmann et al. 2014; Franke et al. 2017).

152   Both sections expose Late Frasnian to Late Famennian deposits, although with a

153   gap during the earliest Famennian in BU. Their stratigraphical context has been formerly

154   described (Girard et al., 2014, 2017) using the zonation of Ziegler and Sandberg (1990);

155   and has been updated applying the zonation of Spalletta et al. (2017) in this study (Fig.

156   2). The CT section (Girard et al., 2014) is ca. 80 m thick. It consists of fine-grained

157   bioclastic limestones from the *Palmatolepis rhenana* to the *Pa. glabra pectinata*

158   conodont Zone, followed by typical reddish griottes from the *Pa. rhomboida* to the *Pa.*

159   *marginifera marginifera* Zone. Lime mudstones were deposited from the *Pa. marginifera*

160   *utahensis* to the *Pa. rugosa trachytera* Zone and are overlain by wackestones with an age

161   from the *Polygnathus styriacus* to the middle of the *Bispathodus ultimus* Zone. The

162   Famennian carbonate deposits are overlain by the Hangenberg shales. Depositional

163   environments ranged from mid to outer ramp. The BU section is ca. 35 m thick and

164   consists of lime mudstones and fine-grained turbiditic wackestones from the *Pa.*

165   *rhenana* to the *Scaphignathus velifer velifer* Zone, followed by nodular limestones of the

166   *Pa. rugosa trachytera* to the middle of the *Bispathodus ultimus* Zone and the Hangenberg

167   shales. Depositional environments ranged from distal slope to outer ramp (Girard et al.,

168   2017).

169

3. Materials

171   Sixty-four and forty samples were collected from the CT and BU sections,
172 respectively (Supplementary Table). Thin sections were used for microfacies analysis.
173 Conodonts were extracted by dissolving a fraction of the samples using 10% formic acid.
174 All conodonts were manually picked from the insoluble residues and determined at the
175 generic and species level. The taxonomic identification allowed establishing a detailed
176 biostratigraphic scheme. The abundance of conodonts is high to exceptionally high, with
177 about 600 platform elements per kg at CT and about 7000 platform elements per kg at
178 BU. Entire and broken platform elements representing at least half of an element were
179 counted per genus to characterize conodont biofacies in each sample (Sandberg, 1976).
180 A fraction of these conodonts was thereafter used for oxygen isotope analyses. All
181 approaches (microfacies, conodont biofacies, and oxygen isotope geochemistry) were
182 performed on the same rock sample.

183

4. Methods

185 *4.1. Age model*

186   The stratigraphy of Late Devonian deposits is mostly based on conodont
187 biostratigraphy. A revised global standard of the Famennian (Late Devonian) conodont
188 zonation has been recently published (Spalletta et al., 2017). Zonal boundaries and
189 duration are essentially identical to those of Ziegler and Sandberg (1990), which was
190 used in the Global Time Scale 2012 (Becker et al., 2012) to date in absolute ages some
191 zonal boundaries. In this study, the zonal boundaries dated in the Global Time Scale
192 2012 were used as anchor points to establish local linear regressions between absolute
193 age and depth along the sections, thus providing age estimates for each sampled level.
194 Anchor points are the basis of the following zones: *Palmatolepis triangularis, Pa. crepida*,
195 *Pa. rhomboidea*, *Pa. marginifera marginifera*, *Pa. rugosa trachytera*, *Polygnathus*
196 *styriacus*, *Palmatolepis gracilis expansa* (adapted to the zonation of Spalletta et al. 2017),
197 and the base of the Early *praesulcata* sensu Ziegler and Sandberg (1990).

198

199 *4.2. Sedimentary facies description*

200   The description of the sedimentary facies in the Col des Tribes and Buschteich
201 sections has been published by Girard et al. (2014) and Girard et al. (2017), respectively.

202 The different facies were characterized by the sedimentological and biological features

203 from outcrops as well as thin sections, allowing an interpretation of the different

204 depositional settings. For each section, this led to an ordering ('score') of the different

205 samples along a theoretical proximal-distal gradient. In order to compare BU and CT, the

206 scoring of the sedimentary facies (later on in the text: 'facies') in the two outcrops have

207 been compiled into a single scheme.

208

209 *4.3. Oxygen isotope analyses*

210 Oxygen isotope ratios of conodont apatite can be used as a paleotemperature

211 proxy (Joachimski and Buggisch, 2002; Joachimski et al., 2009; Luz et al., 1984). Twenty-

212 seven conodont samples from the Buschteich section and 26 conodont samples from the

213 Col des Tribes section have been studied for oxygen isotopes. Chemical conversion of

214 apatite bound phosphate into trisilverphosphate (Ag_3PO_4) was performed according the

215 method described in Joachimski et al. (2009). Oxygen isotope analyses were performed

216 using a TC-EA (high-temperature conversion-elemental analyzer) coupled online to a

217 ThermoFinnigan Delta V Plus mass spectrometer. 0.2 to 0.3 mg Ag_3PO_4 was weighed into

218 silver foil and transferred to the sample carousel of the TC-EA. At 1450 °C, the silver

219 phosphate is reduced and CO forms as the analyte gas (Vennemann et al., 2002). CO was

220 transferred in a helium stream through a gas chromatograph via a Conflo III interface to

221 the mass spectrometer. All values are reported in ‰ relative to V-SMOW. Samples as

222 well as standards were generally measured in triplicate. The measurements were

223 calibrated by performing a two-point calibration (Paul et al., 2007) using NBS 120c

224 ($\delta^{18}O$ = 21.7‰) and a commercial Ag3PO4 (9.9‰). A laboratory standard was used as a

225 control standard and processed together with the samples. All standards were

226 calibrated to TU1 ($\delta^{18}O$ = +21.11‰) and TU2 (+5.45‰; Vennemann et al., 2002). The

227 average oxygen isotope composition of the internationally distributed standard NBS

228 120c was measured as +21.67 ± 0.09 (1 σ; n= 5).

229

230 *4.4. Conodont biofacies*

231 Late Devonian conodont taxa were supposed to have different water depth

232 preferences (Klapper and Barrick, 1978; Seddon and Sweet, 1971). Hence, the

233 proportion of the different genera within a given assemblage was interpreted as a proxy

234 of water depth (Sandberg, 1976; Seddon and Sweet, 1971). Refined biofacies

235   interpretations based on conodont subgenera or even species have been proposed (e.g.

236   Lüddecke et al., 2017) but due to species evolution and replacement through time, this

237   approach appeared difficult to apply to the relatively long record considered in the

238   present study. During the late Frasnian to late Famennian, at least seven genera are

239   present and can provide information about depositional environments (e.g. Corradini,

240   2003; Morrow, 2000; Sandberg, 1976; Seddon and Sweet, 1971). The genera that have

241   been most clearly associated to water depth preferences are the following. (1) For deep

242   waters, *Palmatolepis* and *Bispathodus/Branmehla/Mehlina*. It should be noted that

243   whereas *Palmatolepis* is considered to be a specialist of offshore environments,

244   *Bispathodus* presents wider tolerance to water depth and/or proximity to the shore

245   (Ziegler and Sandberg 1984). (2) *Polygnathus* for intermediate water depth. (3) *Icriodus,*

246   *Scaphignathus,* and *Alternognathus* for shallow waters. Due to their low abundance and

247   similar environmental preferences, the two latter genera have been grouped for

248   biofacies representation. Hence, in this study, the following biofacies were recognized:

249   the palmatolepid biofacies, the palmatolepid-polygnathid biofacies, and the bispathodid-

250   polygnathid biofacies.

251

252   *4.5. Data analysis and statistics*

253   The proportion of each genus was estimated in each sampled level based on

254   counting (Girard et al., 2014, 2017). The description of these proportions corresponds to

255   the conodont biofacies analysis itself. A principal component analysis (PCA on the

256   variance-covariance matrix) was performed on these percentages to summarize the

257   variation of all genera on few main axes. This analysis also provided a representation of

258   the records of CT and BU on the same synthetic axes, allowing a direct comparison of the

259   biofacies variations in the two outcrops. The contribution of each genus percentage to

260   the axes allowed their interpretation in relation to the biofacies. The PCA was performed

261   using the R package ade4 (Dray and Dufour, 2007). The different proxies (microfacies,

262   oxygen isotope ratios and the first axis of the PCA on the conodont percentages) were

263   compared using linear regression analysis in CT and BU separately, and in the combined

264   dataset (CT+BU). To test for a secular climate evolution, the relationship between

265   oxygen isotope values and time was tested using linear regressions in CT, BU and

266   CT+BU. In addition, this relationship was also investigated using a linear model

267   including as terms the age of the levels, the section and the interaction between the two

268 former terms. If the interaction between two terms, here age and section, is significant,

269 this means that the relationship of the dependent variable (here, δ^{18}O values) to age

270 have a different slope in the two sections. To test if δ^{18}O values were different in two

271 phases of the record, t-tests were also used. All these tests were performed under R (R

272 Core Team, 2017). An analysis of variance (ANOVA) on a linear model combining

273 microfacies and oxygen isotopes as explanatory variables was used to assess their

274 relative influence on conodont assemblages, estimated by the scores along the first axis

275 of the PCA on conodont percentages. A type II ANOVA was used, because this method is

276 invariant to ordering of the model terms and is powerful even with unbalanced datasets.

277 This test was done using the R package ffmanova (Langsrud and Mevik, 2012).

278

279 **5. Results**

280 *5.1. Age model*

281 The absolute ages estimated in Becker et al. (2012) for some zonal boundaries

282 served us as anchor points. A correlation with sediment thickness allowed establishing

283 an age model for each section (Fig. 2). The observed sediment thickness includes post-

284 depositional processes such as compaction, erosion, and diagenesis, that may affect the

285 estimates of accumulation rates through time and between sections. With this limitation,

286 Famennian mean accumulation rates were low in CT (5 to 7 mm/kyr^{-1}) and extremely

287 low in BU (1 to 3 mm/kyr^{-1}). Two periods of more or less constant accumulation rates

288 can be identified in BU: one from the *Pa. crepida* Zone to the *Sc. velifer velifer* Zone, and a

289 second, with even lower rates, from the *Palmatolepis rugosa trachytera* Zone to the end

290 of the Famennian. In CT, these two intervals can also be recognized, with possibly a

291 temporary acceleration of deposition during the *Pa. marginifera marginifera* and

292 *marginifera utahensis* Zones. The ages estimated for each sample were thereafter used

293 to plot the variations of the conodont assemblages and of the environmental proxies.

294 This allowed a comparison of the timing of changes in both sections.

295

296 *5.2. Sedimentary facies*

297 The sedimentary facies of BU and CT have been compiled into a single scheme.

298 Five facies types have been distinguished based on microfacies and faunal content (Fig.

299 3). The interpolated scheme is summarized below and compared to the published facies

300 at CT (Girard et al., 2014) and BU (Girard et al., 2017). Details are provided in the Supp.

301   Table 1. Based on these facies characteristics, the temporal variation in the depositional

302   setting can be reconstructed. Note that all depositional environments are relatively

303   deep, and correspond to the deepest environments found on the shelf, and that the

304   terms 'shallow' and 'deep' are used in the context of relative shallowing or deepening. At

305   BU only minor variations can be observed (Fig. 4A). The depositional environment,

306   mostly corresponding to Facies 2, remained relatively deep throughout the record.

307   Intervals with the even deeper Facies 1 can be identified during the Late Frasnian, the

308   *Pa. crepida and termini* Zones, the *Pa. marginifera marginifera* Zone, the *Sc. velifer velifer*

309   Zone, and the top of *Bispathodus ultimus* Zone. The CT section shows evidence for more

310   important changes in water depth. A first shallowing episode occurred during the latest

311   Frasnian and earliest Famennian, followed by a second, shallower episode during the *Pa.*

312   *gracilis gracilis* and the *Pa. marginifera marginifera* Zones. From the top of the

313   *Pseudopolygnathus granulosus* Zone to the end of the Famennian, conditions were

314   constantly shallower than during the two former episodes. These shallowing trends are

315   separated by two deepening episodes, from the *Pa. minuta minuta* to the *Pa. rhomboidea*

316   Zone and from the *Pa. marginifera marginifera* to the *Pseudopolygnathus granulosus*

317   Zone.

318

319   *5.3. Oxygen isotopes*

320   Oxygen isotope ratios measured on conodont apatite from CT are between +17.1

321   and +17.7‰ from the end Frasnian to the *Pa. crepida* zone (Fig. 4B). Values thereafter

322   more or less gradually increase to values around 18‰ in the *Pa. marginifera utahensis*

323   Zone. From the *Sc. velifer velifer* to the *Pa. gracilis expansa*, $\delta^{18}O$ increases to values

324   above +19‰. A slight decrease is observed to the end of the Famennian. Oxygen isotope

325   values of conodont apatite from BU are generally higher than values observed at CT.

326    $\delta^{18}O$ values range from +16.4 to +16.9 ‰ from the end Frasnian to the *Pa. crepida* zone.

327   From a minimum of +16.4 ‰ at the base of the *Pa. crepida* Zone, a trend to higher

328   values occurs up to the *Pa. marginifera marginifera* Zone, reaching $\delta^{18}O$ values of +17.8

329   ‰. A brief decrease marks the first part of the *Pa. marginifera utahensis* Zone, with $\delta^{18}O$

330   values of around +16.7 ‰. Thereafter, up to the end of the Famennian, $\delta^{18}O$ values

331   remain close to +17.5 ‰.

332 The offset in $\delta^{18}O$ between the two sections is relatively small (+0.5 to +1‰) from the

333 *Pa. crepida* Zone to *Pa. marginifera utahensis* Zone, but increases after the *Sc. velifer*

334 *velifer* Zone (+1 to +1.5 ‰). This difference in $\delta^{18}O$ translates into +6 to +6.5°C cooler

335 temperatures in CT in case the offset is solely explained by temperature.

336

337 *5.4. Conodont biofacies*

338 The conodont biofacies follow overall comparable trends in both sections (Fig. 5;

339 Supp. Table 1), sharing a dominance of *Palmatolepis* for most of the time up to a

340 maximum at the base of the *Pa. marginifera marginifera* Zone (up to more than 95% of

341 the assemblage), followed by a progressive decrease towards the end Famennian. This

342 decrease of *Palmatolepis* was compensated almost exclusively by a rise of *Bispathodus* in

343 CT and by a rise of both *Polygnathus* and *Bispathodus* in BU. The Frasnian assemblages

344 were complemented by the occurrence of other genera such as *Polygnathus* and

345 *Ancyrodella*. The *Pa. triangularis* to *Pa. minuta minuta* Zones, which are missing in BU,

346 were marked by an increase in the abundance of *Icriodus* in CT. Another maximum in the

347 abundance of *Icriodus* in CT is recognized in the *Pa. glabra prima* Zone. Except for the *Pa.*

348 *crepida* Zone, *Icriodus* was rare in BU. In CT, a short-term rise of

349 *Scaphignathus/Alternognathus* occurred around the *Ps. granulosus* Zone. A similar but

350 more discrete rise is present at the base of the *Pa. rugosa trachytera* Zone in BU.

351

352 *5.5. Multivariate analysis of the conodont taxa abundances*

353 The principal component analysis performed on the proportions of the different

354 genera allowed summarizing the biofacies variations on one main axis (PC1) expressing

355 more than 75% of the total variance. The record of the two sections CT and BU can be

356 directly compared on these axes. The contribution of the variables (here, the

357 percentages of the different genera) to the axes (Fig. 6A) shows that positive values

358 along the first axis correspond to a high proportion of *Palmatolepis* whereas negative

359 values correspond to a high proportion of *Bispathodus.* Variations along the PC1 axis

360 thus correspond to the replacement of *Palmatolepis* by *Bispathodus*. The second axis

361 represents only less than 20% of variance, and mostly corresponds to variations in the

362 proportion of *Polygnathus*. Other genera contribute very little to the two main axes, due

363 to their rare occurrence in the records.

364   Representing the different levels in the first principal plane of this PCA allows for

365   a comparison of BU and CT conodont biofacies variations (Fig. 6B-I). Most of the time,

366   the range of values covered by samples from the two sections largely overlaps. The

367   oldest samples (mostly Frasnian) are characterized by a peculiar diagonal distribution

368   (Fig. 6B). Their shift in the PCA space compared to Famennian samples is due to the

369   occurrence of genera such as *Ancyrodella* that went extinct during the Frasnian -

370   Famennian crisis. Early Famennian levels of both sections are tightly clustered, sharing

371   extreme positive values along the first axis, due to the overwhelming dominance of

372   *Palmatolepis*.

373   In CT, a shift towards negative PC1 values is launched between the *Pa.*

374   *marginifera marginifera* and *Pa. marginifera utahensis* Zones (Fig. 4C, 6E),

375   corresponding to the onset of the decrease in the abundance of *Palmatolepis* (Fig. 5).

376   This shift went on to reach extreme negative PC1 values as early as the *Po. styriacus*

377   Zone (Fig. 6G, H). This change started more or less at the same time at BU, but it did not

378   occur in a consistent manner for a while. Only towards the end of the studied interval,

379   during the *Bispathodus ultimus* Zone, PC1 values in BU reach a range similar to the one

380   observed in CT (Fig. 6I). This corresponded to the final decrease of *Palmatolepis* at BU,

381   close before its extinction near the Devonian-Carboniferous boundary (Fig. 5). The

382   consequence of this delay in the decrease of *Palmatolepis* at BU was a temporary offset

383   between the two records of conodont genera proportions, starting during the *Ps.*

384   *granulosus* Zone and persisting until the base of the *Bi. ultimus* Zone (Fig. 4C).

385

386   *5.6. Comparison of paleoenvironmental proxies and conodont biofacies*

387   As a first step, we compared the different proxies (Table 2). Facies, oxygen

388   isotope ratios, and the first axis of the principal component analysis on the conodont

389   percentages (later on mentioned as conodont PC1) are all significantly correlated when

390   considering the total dataset (CT+BU). In contrast, none of the correlations is significant

391   when considering BU. At CT, conodont PC1 is significantly correlated to facies and $\delta^{18}O$,

392   but the two latter variables are not correlated.

393   The variation in the oxygen isotope ratios shows a significant secular trend, the

394   relationship of $\delta^{18}O$ and age being significant in the CT, BU and CT+BU datasets.

395   In the linear model investigating the variation of $\delta^{18}O$ depending on age in the two

396   sections, the interaction term between $\delta^{18}O$ and age is not significant. This means that

397   the slope of the regression is the same in the two sections. While the two sections

398   display a similar increase in $\delta^{18}O$ when considering the whole record, from the end

399   Frasnian to the Late Famennian, the records of CT and BU do not follow a similar pattern

400   after the *Pa. marginifera utahensis* Zone (Fig. 4B). The oxygen isotope ratios increase in

401   CT but remain stable in BU. To test for such a discrepancy between the records of the

402   two sections, we performed t-tests between oxygen isotope values of the period

403   preceding and following the apparent shift in CT. The difference in $\delta^{18}O$ is indeed

404   statistically significant in CT (t-test [from *Pa. rhomboidea to Sc. velifer velifer*, n =8] vs.

405   [from *Pa. rugosa trachytera* to *Bi. ultimus*, n = 7], P = 0.0026). In contrast, the $\delta^{18}O$ values

406   of the same periods do not differ in BU (t-test [n = 6 and 11], P = 0.3443).

407   Finally, to investigate whether $\delta^{18}O$ or facies better explains the variation of the

408   conodont genera, linear models with conodont PC1 as dependent variable, and $\delta^{18}O$ and

409   facies as independent factors were considered (Table 3). The interaction term between

410   both factors ($\delta^{18}O$ and facies) is weak (p = 0.0311 for CT+BU) or not significant (for CT

411   and BU separately). This term was therefore discarded from the models. Facies and $\delta^{18}O$

412   are significant explanatory variables of conodont biofacies when considering CT and BU

413   together, and CT alone. Facies explains more than three times more variance than $\delta^{18}O$

414   in both cases. None has significant effect in BU.

415

416   **6. Discussion**

417   Our detailed oxygen isotope records generally show an increase in $\delta^{18}O$ in both

418   sections from the end Frasnian to end Famennian, coherent with described global

419   cooling during this time interval (Joachimski et al., 2009). However, in details, the two

420   records show different temperature variations from the *Pa. rugosa trachytera* Zone to

421   end Famennian. While temperature remained more or less stable throughout the

422   Famennian in the BU section (Saxo-Thuringia), it decreased in the CT section (Montagne

423   Noire) towards *Sc. velifer velifer* Zone. This difference in $\delta^{18}O$ between CT and BU is

424   mirrored by different sea-level variations in CT and BU, as pointed out by facies

425   description. Given these differences between the paleoenvironmental settings of the two

426   areas, conodont biofacies delivered remarkably similar records, questioning the role of

427   the paleoenvironmental forcing on conodont assemblages.

428

429   *6.1. Paleotemperature variations: a global trend mitigated by paleogeography?*

430   A global temperature trend has been sketched for the Late Devonian (McGhee,

431   2013), based on variations in $\delta^{18}O$ of conodont apatite (Joachimski et al., 2009). This

432   composite record showed a rapid succession of cooling and warming pulses around the

433   Frasnian-Famennian boundary (Balter et al., 2008; Joachimski and Buggisch, 2002;

434   Huang et al. 2018). After a warm period during the *triangularis* Zone, a progressive long-

435   term cooling was proposed for the rest of the Famennian (Joachimski et al., 2009),

436   culminating into a period with stable ice caps during the early Carboniferous (Buggisch

437   et al. 2008). As for some other oxygen isotope studies in the Paleozoic, our isotope

438   records are based on conodont apatite, thus tracing the environment where the

439   conodont lived. Furthermore, all analyses were performed on the same genus,

440   *Palmatolepis*, avoiding the problem that different oxygen isotope values in the two

441   sections may be due to analyses on genera with different habitat preferences. Our

442   results support a long-term cooling, since the two sections displayed a parallel increase

443   in the oxygen isotope ratio from the end Frasnian to end Famennian, although more

444   pronounced in CT than in BU. An offset, however, exists between the records of the two

445   sections, with BU constantly showing lower $\delta^{18}O$ values than CT. Based on the

446   paleogeographic reconstruction (Fig. 1), BU and CT were both in the subtropical zone.

447   The constant offset between the two records can thus hardly be explained by a

448   latitudinal difference. Possibly, CT being positioned further towards the Paleotethys

449   (Franke et al., 2017), it might have been more exposed to the colder water masses of the

450   open Paleotethys Ocean and Paleo-Adria epicontinental sea.

451   Beyond the cooling trend registered in both sections from the *Pa. crepida* to *Pa.*

452   *marg. marginifera* Zone, the oxygen isotope records from BU and CT show differing

453   trends after the *Pa*. *marginifera utahensis* Zone. This pattern is also seen in other

454   sections studied by Joachimski et al. (2009). For example, in the La Serre section

455   (Montagne Noire) an increase in $\delta^{18}O$ is reported between the *marginifera marginifera*

456   and *Sc. velifer velifer* Zones, similar and synchronous to the one documented in CT. In

457   contrast in the Kahlleite section (Saxo-Thuringian area) $\delta^{18}O$ is relatively stable as in BU

458   (Fig. 4). The difference in the $\delta^{18}O$ records of the BU and CT sections after the *Pa.*

459   *marginifera utahensis* Zone is thus confirmed at the regional scale, suggesting that the

460   paleogeographic position of the two microcontinents may have controlled the

461   temperature changes.

462   Paleogeographic reconstructions suggest that Saxo-Thuringia was located close

463   to the first zone of closure of the Rheic Ocean (Franke et al., 2017). As the closure of the

464   Rheic Ocean progressed during the Famennian, the area might have been influenced by

465   a relative restriction of the water masses exchanges between the Rheic Ocean and the

466   Paleotethys Ocean. The upper water column temperatures might have been warmer

467   than in the open sea, as e.g. nowadays in the Caribbean Sea, the Persian Gulf, or the

468   eastern Mediterranean (see for instance Schlitzer, 2006; Schmidt et al., 2016),

469   dampening the effects of the global cooling, especially in a subtropical area. In contrast,

470   the CT section and more generally the Armorica area, being opened towards the

471   Paleotethys Ocean, would have been exposed to the Paleotethys water circulation and

472   global temperature trends, as established by Joachimski et al. (2009). This

473   interpretation is corroborated by the fact that Late Famennian $\delta^{18}O$ values recorded in

474   the Carnic Alps (Paleo-Adria, Fig. 1; *Pa. gracilis expansa* and *Bi. ultimus* Zones: ~18,3 ‰;

475   Kaiser et al., 2006, 2008), and hence also in an environment open towards the

476   Paleotethys (Paleo-Adria on Fig. 1), were closer to those recorded at CT than at BU.

477

478   *6.2. Water depth variations, combination of eustatic trends and local tectonics*

479   Sea-level variations correspond to a high-stand during the end of the Frasnian,

480   followed by a progressive sea-level fall during the Famennian (Haq and Schutter, 2008;

481   Johnson et al., 1985, 1996; Sandberg et al., 2002). These variations appear to have

482   occurred world-wide, thus pointing to eustatic trends (Johnson et al., 1985, 1996). In

483   this context, a decrease in water depth should coincide with increasing ice volume, a

484   glacio-eustatic sea-level fall and a temperature decrease. In the CT section, a regressive

485   trend and a cooling are indeed registered, but they do not occur in parallel with the

486   shallowing clearly postponing the shift towards colder temperature. Another

487   discrepancy with the expectation is that both the temperature and water depth decrease

488   do not seem to have occurred in a progressive manner, but rather abruptly. Possibly,

489   paleogeographic and/or tectonic events might have temporarily mitigated the

490   expression of the long-term trend in CT. Water depth variations in BU do not follow this

491   global trend. In BU, the depositional environment remained deep throughout the

492   Famennian, and tectonic activity has been invoked to explain this discrepancy (Girard et

493   al., 2017). The paleogeographic position of Saxo-Thuringia, close to Baltica and hence

494   one of the first microcontinent to collide with it, matches well with active tectonics

495   causing a local departure from the eustatic trend.

496

497   *6.3. Congruent variations of the conodont assemblages despite discrepant*

498   *paleoenvironmental settings*

499   In contrast to the different patterns of temperature variation after the *Pa.*

500   *marginifera utahensis* Zone, and differences in water depth records in CT and BU, trends

501   in conodont biofacies are quite comparable. Both sections reflect a dominance of

502   *Palmatolepis* for most of the Famennian with a decline starting in the *Pa. marginifera*

503   *marginifera* Zone. If the difference between the environments at CT and BU had any

504   impact on the conodont assemblages, it was only minor and corresponded to a transient

505   offset between the two conodont records. However, conodont biofacies are advocated to

506   be mostly driven by water depth variations, due to the habitat preferences of the

507   different conodont genera (Sandberg, 1976; Seddon and Sweet, 1971). Initially, two

508   ecological models, i.e. depth stratification vs. lateral segregation, were proposed

509   (Klapper and Barrick, 1978; Seddon and Sweet, 1971). The depth-stratification model

510   implies that specific conodont taxa inhabited different depth zones within the water

511   column, whilst the lateral segregation model proposes that bottom-dwelling taxa were

512   dominantly controlled by habitat properties near the sediment–water interface. The

513   abundant occurrence of conodonts during anoxic events precludes a benthic or

514   nektobenthic lifestyle. During the Frasnian and the Famennian, genera supposed to have

515   "shallow preferences "(e.g. *Icriodus*) and "preferences for deep environments" (e.g.

516   *Palmatolepis*) have been shown to share similar oxygen isotope signatures, suggesting

517   that they were living in the same water-mass (Joachimski et al., 2009). This supports the

518   interpretation that all genera were at that time living close to the surface, but occupying

519   proximal or distal locations. The higher proportion of the offshore surface dweller genus

520   *Palmatolepis* in the sediments from BU than from CT is coherent with the more off-shore

521   depositional setting in BU. The decrease of the genus *Palmatolepis* after the *Pa.*

522   *marginifera marginifera* Zone is also coherent with the regressive trend characterizing

523   the Famennian. Possibly, before the *Sc. velifer velifer* Zone, water depth was constantly

524   deep enough to favor the dominance of this offshore surface dweller genus. However, if

525   a direct forcing of water depth on conodont distribution is assumed, conodont biofacies

526   at BU should have been relatively stable through time, and depart more clearly from the

527 trend observed at CT. This suggests that the response of conodont assemblages to water

528 depth was mitigated by other factors. Possibly, the eustatic regressive trend was

529 disadvantageous to the offshore surface dweller genus *Palmatolepis* at a worldwide

530 scale, triggering its global decline. Ultimately, it would have even declined in constantly

531 deep environments such as BU, although with a time lag suggesting that it temporarily

532 found there a refuge of favorable environments.

533

534 *6.4. Relationship between the different paleoenvironmental proxies*

535   The three paleoenvironmental proxies considered here (sedimentary facies,

536 oxygen isotopes, and conodont biofacies) are potentially interrelated: oxygen isotopes

537 are temperature proxies; facies traces water depth and distance to the shore, related to

538 temperature trends through eustatic variations; and conodont biofacies are interpreted

539 as related to water depth due to habitat preferences of the different conodont genera

540 along a proximal-distal gradient in the surface waters. No relationship between these

541 proxies is evident in BU, but this absence of a significant correlation is probably due to

542 the reduced range of variation in the oxygen isotope ratios and facies observed in this

543 section. Oxygen isotopes and facies are correlated when considering the total data set.

544 However, conodont PC1 displays a stronger relationship with oxygen isotopes on the

545 one hand, and with facies on the other hand, than oxygen isotopes with facies: the

546 percentage of variance explained is larger, leading to significant relationships in CT as

547 well (Table 2). Considering the percentage of variance explained, facies furthermore

548 appears as a better explanatory variable for conodont variations than $\delta^{18}O$. The

549 sedimentary facies trace directly the depth of the depositional environment but the

550 relevance of this approach has been discussed due to the paucity of preserved biotas in

551 old sediments (e.g. see Flügel, 2004; Lüddecke et al., 2017). The correlation evidenced

552 between facies and conodont biofacies is nevertheless coherent with the interpretation

553 of conodont genera distribution being controlled by water depth, along a proximal-distal

554 gradient (Klapper and Barrick, 1978). The fact that conodont biofacies respond earlier

555 and more progressively to the global regressive trend may be due to the fact that CT and

556 BU being located in outer shelf environments, the decrease in water depth should be

557 important enough to cause a change in the facies.

558

559 *6.5. Paleogeography and paleoenvironment: a complex interplay*

560   Many studies focused on global environmental trends in the Devonian (e.g.

561   Goddéris and Joachimski, 2004; Haq and Schutter, 2008; Miller et al., 2005; Sandberg et

562   al., 1988; Wilson and Norris, 2001), especially during the Late Devonian for which

563   environmental conditions have been suggested to be homogeneous within the

564   subtropical zone, and the marine faunas to be cosmopolitan. However, our results, based

565   on two detailed 13 My long records, indicated different paleoenvironmental changes in

566   BU and CT. After the end of the *Pa. marginifera utahensis* Zone, the cooling and the

567   regressive trend found little expression in BU compared to CT, but these differences are

568   only weakly mirrored in the conodont assemblages. The differences in the temperature

569   records of CT and BU are not only observed in the two studied sections, but registered

570   as well in two other sections (Kahlleite and La Serre) from the Saxo-Thuringian and

571   Montagne Noire areas (Joachimski et al., 2009), respectively. We propose that the

572   deviation of the BU record from what we interpret as the global trend may be attributed

573   to the paleogeography of the Saxo-Thuringian area, where a progressive restriction of

574   water-mass exchange possibly accompanied the closing of the seaway between the

575   remnant Rheic and Paleotethys oceans. This restricted paleogeography together with a

576   subtropical location might have favored the persistence of warm conditions in the sea-

577   waters where conodonts lived despite the onset of global cooling. Such setting should

578   also have been prone to active tectonics overprinting the eustatic trend. Not mutually

579   exclusive, the closure of the Rheic Ocean itself might have contributed to the global

580   climate change, by interrupting the circum-equatorial circulation (see for instance for

581   the closure of the Panama Isthmus: Bartoli et al., 2005 and Haug and Tiedemann, 1998),

582   but this remains speculative and challenges further studies.

583   Increasing the geographic coverage of a multi-proxy approach, such as the one

584   outlined here, may thus provide relevant information to better constrain

585   paleogeographic reconstructions characterized by a complex distribution of land and

586   water masses, as e.g. in the Late Devonian. This key step will contribute to a better

587   understanding of the complex interplay between paleogeography, climate, and biotic

588   response and go beyond the tempting, but misleading, view of global trends affecting the

589   different regions in a relatively homogeneous manner.

590

591   **7. Conclusions**

592   This study presents a detailed comparison of two Famennian successions in the

593 Montagne Noire (France) and Saxo-Thuringia (Germany). During the Famennian, both

594 areas were located in the subtropical realm and were part of two microcontinents

595 bracketed between the remnant Rheic Ocean and Gondwana. Based on the same rock

596 samples, paleotemperatures were estimated using oxygen isotopes of conodont apatite,

597 depositional environments were assessed based on sedimentary facies, and the

598 response of conodont assemblages was evaluated using conodont biofacies. Applying a

599 principal component analysis to biofacies data provided a synthetic axis summarizing

600 the biofacies variations along the two sections. This allowed for a quantitative

601 comparison of the biofacies records with paleoenvironmental proxies.

602   During the Famennian, both the Montagne Noire and Saxo-Thuringia display a

603 parallel increase in the oxygen isotope ratios translating into long-term cooling.

604 However, during the Late Famennian, temperatures remained stable in Saxo-Thuringia,

605 leading to a temperature offset compared to the Montagne Noire record. The Late and

606 latest Famennian are also characterized by a regressive trend which was found to be

607 well expressed in the sedimentary facies in the Montagne Noire, but not in Saxo-

608 Thuringia, where the depositional environment remained deep throughout. Despite

609 these environmental differences, conodont biofacies were rather comparable in the

610 Montagne Noire and Saxo-Thuringia. A temporary offset however suggested that

611 *Palmatolepis*, the typical off-shore surface dwelling taxon, was abundant for a longer

612 time period in the deep Saxo-Thuringian environment. The environmental differences

613 between the two areas are tentatively explained by their paleogeographic location. The

614 Saxo-Thuringian microplate is interpreted as located close to the point of first closure of

615 the Rheic Ocean and thus might have been influenced by active tectonism and a

616 restricted water mass exchange, blurring the impact of the long-term trends in this

617 setting.

618

Acknowledgments

625
626 **References**
627

628 Balter, V., Renaud, S., Girard, C., Joachimski, M.M., 2008. Record of climate-driven

629   morphological changes in 376 Ma Devonian fossils. Geology 36, 907-910.

630 Bartoli, G., Sarnthein, M., Weinelt, M., Erlenkeuser, H., Garbe-Schônberg, C.-D., Lea, D.W.,

631   2005. Stable isotope analysis and temperature reconstruction data from DSDP Hole 94-

632   609B and ODP Hole 162-984B, Supplement to: Bartoli, G. et al. (2005): Final closure of

633   Panama and the onset of northern hemisphere glaciation. Earth Planet. Sci. Lett., 237,

634   33-44, https://doi.org/10.1016/j.epsl.2005.06.020. PANGAEA.

635 Becker, R.T., 1993. Anoxia, eustatic changes, and upper Devonian to lowermost

636   Carboniferous global ammonoid diversity, in: House, M.R. (Ed.), The Ammonoidea:

637   Environment, Ecology, and Evolutionary Change. Systematics Association Special

638   Volume, Oxford, pp. 115-163.

639 Becker, R.T., Gradstein, F.M., Hammer, O., 2012. The Devonian Period, in: Gradstein, F.M.,

640   Ogg, J.G., Schmitz, M.D., Ogg, G.M. (Eds.), The Geologic Time Scale 2012. Elsevier,

641   Oxford, pp. 559-602.

642 Becker, R.T., House, M.R., 1997. Sea-level changes in the Upper Devonian of the Canning

643   Basin, Western Australia. Cour. Forsch.-Inst. Senckenberg 199, 126-146.

644 Becker, R.T., Kaiser, S.I., Aretz, M., 2016. Review of chrono-, litho- and biostratigraphy

645   across the global Hangenberg Crisis and Devonian–Carboniferous Boundary, in:

646 Becker, R.T., Koenigshof, P., Brett, C.E. (Eds.), Devonian Climate, Sea Level and

647   Evolutionary Events. The Geological Society of London, London, 423, 355-386.

648 Belka, Z., Wendt, J., 1992. Conodont biofacies patterns in the Kellwasser Facies (upper

649   Frasnian/lower Famennian) of the eastern Anti-Atlas, Morocco. Palaeogeogr.

650   Palaeoclimatol. Palaeoecol. 91, 143-173.

651 Brett, C., Allison, P.A., 1998. Paleontological Approaches to the Environmental

652   Interpretation of Marine Mudrocks, in: Schieber, Zimmerle, Sethi (Eds.), Shales and

653   Mudstones. E Schweizerbartsche Verlagsbuchandlung (Nagel u. Obermiller), Stuttgart,

654   pp. 301-349.

655 Buggisch, W., Joachimski, M. M., Sevastopulo, G., Morrow, J.R. 2008. Mississippian $\delta^{13}C_{carb}$

656   and conodont apatite $\delta^{18}O$ records — Their relation to the Late Palaeozoic Glaciation,

657   Palaeogeogr. Palaeoclimatol. Palaeoecol. 268(3-4), 273-292, doi:

658   doi:10.1016/j.palaeo.2008.03.043.

659 Caputo, M.V., Melo, J.H.G., Streel, M., Isbell, J.L., 2008. Late Devonian and Early

660 Carboniferous glacial records of South America, in: Fielding, C.R., Frank, T.D., Isbell, J.L.

661 (Eds.), The Geological Society of America, Special Paper. Geol. Soc. America, pp. 161-

662 173.

663 Corradini, C., 2003. Late Devonian (Famennian) conodonts from the Corona Mizziu

664 Sections near Villasalto (Sardinia, Italy). Palaeontographia Italica 89, 65-116.

665 Dray, S., Dufour, A.-B., 2007. The ade4 package: implementing the duality diagram for

666 ecologists. J. Stat. Softw 22, 1-20.

667 Eckelmann, K., Nesbor, H.-D., Königshof, P., Linnemann, U., Hofmann, M., Lange, J.-M.,

668 Sagawe, A., 2014. Plate interactions of Laurussia and Gondwana during the formation

669 of Pangaea — Constraints from U–Pb LA–SF–ICP–MS detrital zircon ages of Devonian

670 and Early Carboniferous siliciclastics of the Rhenohercynian zone, Central European

671 Variscides. Gondwana Research 25, 1484-1500.

672 Feist, R., Becker, R.T., 1997. Discovery of Famennian trilobites in Australia (Late

673 Devonian, Canning Basin, NW Australia). Geobios M.S. 20, 231-242.

674 Flügel, E., 2004. Microfacies of carbonate rocks. Analysis, Interpretation and Application.

675 Springer Verlag, Berlin, Heildelberg, NewYork.

676 Franke, W., Cocks, L.R.M., Torsvik, T.H., 2017. The Palaeozoic Variscan oceans revisited.

677 Gondwana Res. 48, 257-284.

678 Girard, C., Feist, R., 1997. Eustatic trends in conodont diversity across the

679 Frasnian/Famennian boundary in the stratotype area, Montagne Noire, France. Lethaia

680 29, 329-337.

681 Girard, C., Cornée, J.-J., Corradini, C., Fravalo, A., Feist, R., 2014. Palaeoenvironmental

682 changes at Col des Tribes (Montagne Noire, France), a reference section for the

683 Famennian of north Gondwana-related areas. Geol. Mag. 151, 864-884.

684 Girard, C., Cornée, J.-J., Charruault, A.-L., Corradini, C., Weyer, D., Bartzsch, K., Joachimski,

685 M.M., Feist, R., 2017. Conodont biostratigraphy and palaeoenvironmental trends during

686 the Famennian (Late Devonian) in the Thuringian Buschteich section (Germany).

687 Newsl. Stratigr. 50, 71-89.

688 Goddéris, Y., Joachimski, M.M., 2004. Global change in the Late Devonian: modelling the

689 Frasnian-Famennian short-term carbon isotope excursions. Palaeogeogr.

690 Palaeoclimatol. Palaeoecol. 202, 309-329.

691   Haq, B.U., Schutter, S.R., 2008. A chronology of Paleozoic sea-level changes. Science 322,

692   64-68.

693   Hartenfels, S., 2011. Die globalen Annulata-Events und die Dasberg-Krise (Famennium,

694   Oberdevon) in Europa und Nord-Afrika – hochauflösende Conodonten-Stratigraphie,

695   Karbonat-Mikrofazies, Paläoökologie und Paläodiversität. Münstersche Forschungen

696   zur Geologie und Paläontologie, Paleontologia e Stratigrafia 115, 141-158.

697   Hartenfels, S., Becker, R.T., 2009. Timing of the global Dasberg Crisis – implications for

698   Famennian eustasy and chronostratigraphy. Palaeontographica Americana 63, 71-97.

699   Hartenfels, S., Becker, R.T. 2017. The global Annulata Events: review and new data from

700   the Rheris Basin (northern Tafilalt) of SE Morocco, in: Becker, R.T., Koenigshof, P.,

701   Brett, C. (Eds.), Devonian Climate, Sea Level and Evolutionary Events. Geological

702   Society, London, Special Publications 423, http://doi.org/10.1144/SP423.1.

703   Haug, G.H., Tiedemann, R., 1998. Stable carbon and oxygen isotope ratios of Cibicidoides

704   wuellerstorfi, and CaCO3 and sand content of ODP Hole 165-999A, Supplement to:

705   Haug, GH; Tiedemann, R (1998): Effect of the formation of the Isthmus of Panama on

706   Atlantic Ocean thermohaline circulation. Nature, 393, 673-676,

707   https://doi.org/10.1038/31447. PANGAEA.

708   House, M.R., 1985. Correlation of mid-Palaeozoic ammonoid evolutionary events with

709   global sedimentary perturbations. Nature 313, 17-22.

710   Huang, C., Joachimski, M.M., Gong, Y., 2018. Did climate changes trigger the Late

711   Devonian Kellwasser crisis? Evidence from a high-resolution $\delta^{18}O_{PO4}$ record from South

712   China. Earth Planet. Sci. Letters 495, 174-184.

713   Isaacson, P.E., Dìaz-Martinez, E., Grader, G.W., Kalvoda, J., Babek, O., Devuyst, F.X., 2008.

714   Late Devonian-earliest Mississippian glaciation in Gondwanaland and its

715   biogeographic consequences. Palaeogeogr. Palaeoclimatol. Palaeoecol. 268, 126-142.

716   Joachimski, M., Buggisch, W., 2002. Conodont apatite $\delta^{18}O$ signatures indicate climatic

717   cooling as a trigger of the Late Devonian mass extinction. Geology 30, 711-714.

718   Joachimski, M.M., van Geldern, R., Breisig, S., Buggisch, W., Day, J., 2004. Oxygen isotope

719   evolution of biogenic calcite and apatite during the Middle and Late Devonian. Int. J.

720   Earth Sci 93, 542-553.

721   Joachimski, M.M., Breisig, S., Buggisch, W., Talent, J.A., Mawson, R., Gereke, M., Morrow,

722   J.R., Day, J., Weddige, K., 2009. Devonian climate and reef evolution: Insights from

723   oxygen isotopes in apatite. Earth Planet. Sci. Lett. 284, 599-609.

724 Johnson, J.G., Klapper, G., Sandberg, C.A., 1985. Devonian eustatic fluctuations in
725   Euramerica. Geol. Soc. Am. Bull. 96, 567-587.

726 Johnson, J.G., Klapper, G., Elrick, M., 1996. Devonian transgressive-regressive cycles and
727   biostratigraphy, Northern Antelope Range, Nevada: establishment of reference
728   horizons for global cycles. Palaios 11, 3-14.

729 Kaiser, S.I., Steuber, T., Becker, R.T., Joachimski, M.M., 2006. Geochemical evidence for
730   major environmental change at the Devonian-Carboniferous boundary in the Carnic
731   Alps and the Rhenish Massif. Palaeogeogr. Palaeoclimatol. Palaeoecol. 240, 146-160.

732 Kaiser, S.I., Steuber, T., Becker, R.T., 2008. Environmental change during the Late
733   Famennian and Early Tournaisian (Late Devonian–Early Carboniferous): implications
734   from stable isotopes and conodont biofacies in southern Europe. Geol. J. 43, 241-260.

735 Kaiser, S.I., Aretz, M., Becker, R.T., 2015. The global Hangenberg Crisis (Devonian-
736   Carboniferous transition): a review of a first order mass extinction, in: Becker, R.T.,
737   Königshof, P., Brett, C.E. (Eds.), Devonian climate, sea level and evolutionay events.
738   Geol. Soc. Spec. Publ., London 423, 387-437.

739 Klapper, G., Barrick, J.E., 1978. Conodont ecology: pelagic versus benthic. Lethaia 11, 15-
740   23.

741 Korn, D., 2004. The mid-Famennian ammonoid succession in the Rhenish Mountains: the
742   "*annulata* Event" reconsidered. Geological Quarterly 48, 245-252.

743 Korn, D., De Baets, K., 2015. Biogeography of Paleozoic ammonoids, in: Klug, C., Korn, D.,
744   De Baets, K., Kruta, I., Mapes, R.H. (Eds.), Ammonoid Paleobiology: From
745   macroevolution to paleogeography. Springer, New York, pp. 299-328.

746 Langsrud, Ø., Mevik, B.-H., 2012. ffmanova: Fifty-fifty MANOVA, https://CRAN.R-
747   project.org/package=ffmanova.

748 Lüddecke, F., Hartenfels, S., Becker, R.T., 2017. Conodont biofacies of a monotonous
749   middle Famennian pelagic carbonate succession (Upper Ballberg Quarry, northern
750   Rhenish Massif). Palaeobio. Palaeoenv. 97, 591–613.

751 Luz, B., Kolodny, Y., Kovak, J., 1984. Oxygen isotope variations in phosphate of biogenic
752   apatites, III. Conodonts. Earth Planet. Sci. Lett. 69, 255-262.

753 McGhee, G.R.J., 1996. The Late Devonian Mass Extinction - The Frasnian/Famennian
754   crisis. Columbia University Press, New York.

755 McGhee, G.R., Jr., 2013. When the invasion on land failed: the legacy of the Devonian
756   extinctions. Columbia University Press, New-York.

757 Miller, K.G., Kominz, M.A., Browning, J.V., Wright, J.D., Mountain, G.S., Katz, M.E.,

758   Sugarman, P.J., Cramer, B.S., Christie-Blick, N., Pekar, S.F., 2005. The Phanerozoic

759   Record of Global Sea-Level Change. Science 310, 1293–1298.

760 Morrow, J., 2000. Shelf-to-basin lithofacies and conodont paleoecology across Frasnian-

761   Famennian (F-F, mid-Late Devonian) boundary, Central Great Basin (Western U.S.A.).

762   Cou. Forsch.-Inst. Senckenberg 219, 1-57.

763 Mottequin, B., Brice, D., Legrand-Blain, M., 2013. Biostratigraphic significance of

764   brachiopods near the Devonian–Carboniferous boundary. Geol. Mag. 151, 216-228.

765 Paul, D., Skrzypek, G., Forizs, I., 2007. Normalization of measured stable isotope

766   composition to isotope reference scale – a review. Rapid Comm. Mass Spectr. 21, 3006-

767   3014.

768 R Core Team, 2017. R: A language and environment for statistical computing. R

769   Foundation for Statistical Computing, Vienna, Austria. URL   https://www.R-

770   project.org/.

771 Sandberg, C.A., 1976. Conodont biofacies of late Devonian *Polygnathus styriacus* Zone in

772   western United States, in: Barnes, C.R. (Ed.), Conodont Paleoecology. Geol. Assoc.

773   Canada spec. Pap., Montreal, pp. 171-186.

774 Sandberg, C.A., Ziegler, W., Dreesen, R., Butler, J.L., 1988. Late Frasnian mass extinction:

775   conodont event stratigraphy, global changes, and possible causes. Cour. Forsch.-Inst.

776   Senckenberg 102, 263-307.

777 Sandberg, C.A., Morrow, J.R., Ziegler, W., 2002. Late Devonian sea-level changes,

778   catastrophic events, and mass extinctions. Geol. Soc. America Spec. Pap. 356, 473-487.

779 Schindler, E. 1993. Event-stratigraphic markers within the Kellwasser Crisis near the

780   Frasnian/Famennian boundary (Upper Devonian) in Germany. Palaeogeogr.

781   Palaeoclimatol. Palaeoecol. 104, 115-125.

782 Schlitzer, R., 2006. Ocean data view - 3.1.0. http://odv.awi.de

783 Schmidt, D., Caromel, A., Seki, O., Rae, J.W.B., Renaud, S., 2016. Morphological response of

784   planktic foraminifers to habitat modifications associated with the emergence of the

785   Isthmus of Panama. Mar. Micropaleontol. 128, 28-38.

786 Seddon, G., Sweet, W.C., 1971. An ecologic model for conodonts. J. Paleont. 45, 869-880.

787 Spalletta, C., Perri, M.C., Over, D.J., Corradini, C., 2017. Famennian (Upper Devonian)

788   conodont zonation: revised global standard. Bull. Geosci. 92, 1-27.

789 Stampfli, G.M., Hochard, C., Vérard, C., Wilhem, C., vonRaumer, J., 2013. The formation of
790   Pangea. Tectonophysics 593, 1-19.

791 Vennemann, T.W., Fricke, H.C., Blake, R.E., O'Neil, J.R., Colman, A., 2002. Oxygen isotope
792   analysis of phosphates: a comparison of techniques from analysis for Ag3PO4. Chem.
793   Geol. 185, 321-336.

794 Walliser, O.H., 1996. Global events and event stratigraphy. Springer Verlag, Berlin,
795   Heidelberg, New York.

796 Wilson, P.A., Norris, R.D., 2001. Warm tropical ocean surface and global anoxia during
797   the mid-Cretaceous period. Nature 412, 425-429.

798 Ziegler, W., 1962. Taxionomy und Phylogenie oberdevonischer Conodonten und ihre
799   stratigraphische Bedeutung. Abhandlungen des hessischen Landesamtes für
800   Bodenforschung 38, Wiesbaden, 166p.

801 Ziegler, W., Sandberg, C.A., 1984. *Palmatolepis*-based revision of upper part of standard
802   Late Devonian conodont zonation, in: Clark, D.L. (Ed.), Conodont biofacies and
803   provincialism. Geological Society of American special Paper, Boulder/Colorado, pp.
804   179-194.

805 Ziegler, W., Sandberg, C.A., 1990. The late Devonian standard conodont zonation. Cour.
806   Forsch.-Inst. Senckenberg 121, 1-115.

Figure captions

Figure 1. Paleogeographic reconstruction during the latest Famennian (simplified after Franke et al. 2017). BU: Buschteich; CT: Col des Tribes. Rectangles: investigated areas.
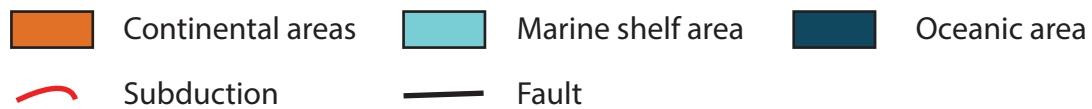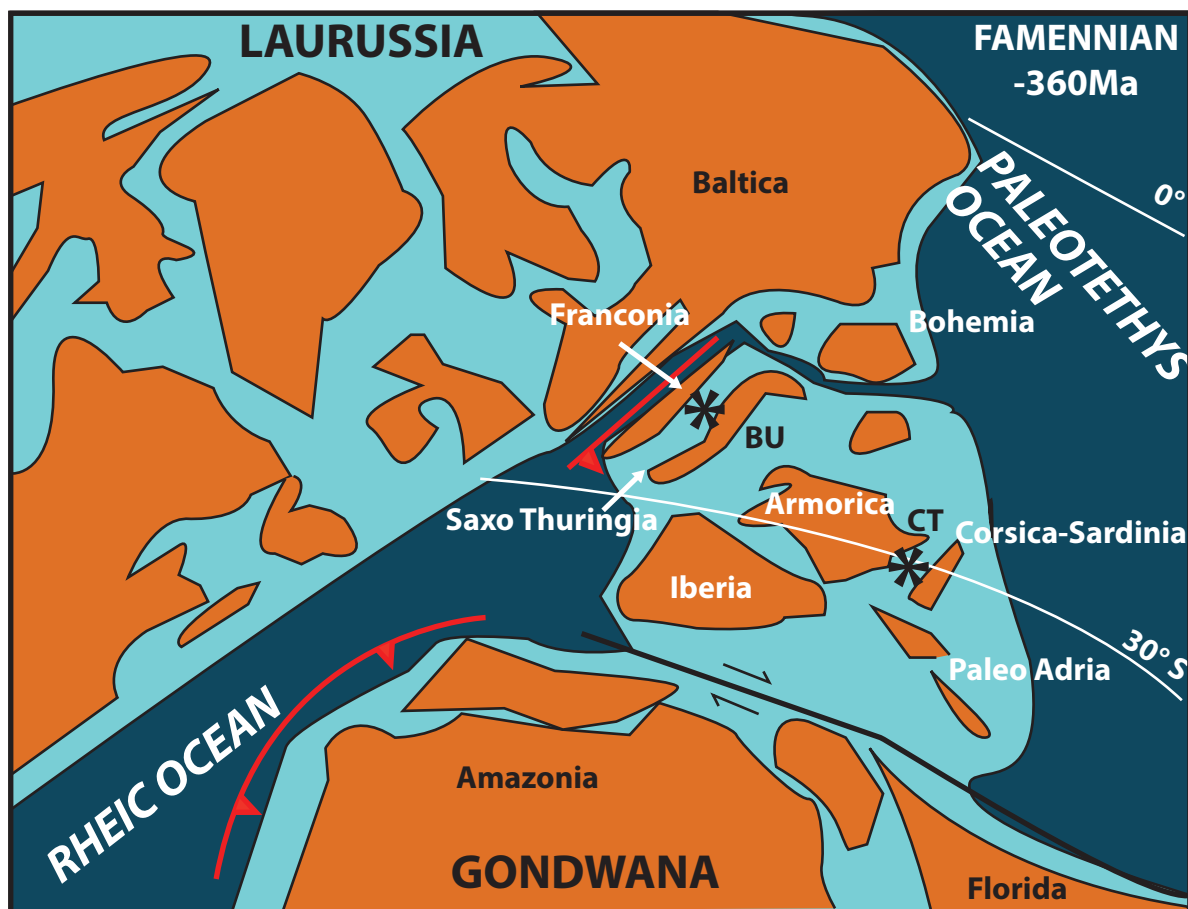
Figure 2. Age model allowing comparison of carbonate production rates between Buschteich (BU; red circles) and Col des Tribes (CT; green diamonds). Depth is given in meters. Conodont zonations according Ziegler and Sandberg (1990) on the right and Spalletta et al. (2017) on the left, absolute ages based on Becker et al. (2012). Each symbol corresponds to a sampled level. FRS: Frasnian. *Pa.*: *Palmatolepis*; *del.*: *delicatula*; *gl.*: *glabra*; *marg.*: *marginifera*; *gr.*: *gracilis*; *Sc.*: *Scaphignathus*; *v.*: *velifer*; *r.*: *rugosa*; *Ps.*: *Pseudopolygnathus*; *Bi.*: *Bispathodus*, *ac.*: *aculeatus.* In grey, zones which were not recognized in both sections.

Figure 3. Depositional model for the Col des Tribes (CT) and Buschteich (BU) sections during the Famennian.

Figure 4. Famennian environmental changes and conodont assemblage variations in the Buschteich section (BU; Saxo-Thuringia) and Col des Tribes section (CT; Montagne Noire). A: Facies distribution for CT and BU from the deepest (1) to the shallowest (5). B: $\delta^{18}O$ in CT and BU samples, compared with data of Joachimski et al. (2009) from Thuringia (Kahlleite, blue circles) and the Montagne Noire (La Serre; grey diamonds). C. Variations of conodont assemblage through time depicted as variations along the first axis of the PCA on conodont genera percentages. Green diamonds: CT; red circles: BU. Abbreviations: see Figure 2.

Figure 5. Conodont biofacies in CT and BU (after Girard et al. 2014; 2017). The proportions have been plotted again the age model. Note the absence of data (Gap) for the *Pa. linguiformis* to *Pa. crepida* zones at BU (white rectangle). *Scaphignathus and Alternognathus*: *Sc., Siphonodella*: *Si.* on the figure.

Figure 6. Principal component analysis of the variations in the percentages of the conodont genera in BU and CT. The first two axes of the PCA are represented (PC1 = 77.5%; PC2 = 18.3%). Upper left panel: contribution of the percentages of the different genera to the first two PC axes. Next panels: distribution of the different levels in the plane defined by the first two PC axes (PC1 = 77.5%; PC2 = 18.3%). The representation has been split by temporal zones (because of their limited sampling, *Pa. triangularis* to *Pa. gl. pectinata* Zones have been grouped). Each dot represents the assemblage in a level. CT: green diamonds, green diamonds with black outlines: levels from the *triangularis* and *minuta minuta* Zones; BU: red circles. *Pa.*: *Palmatolepis*; *gl.*: *glabra*; *gr.*: *gracilis*; *marg.*: *marginifera*; *Sc.*: *Scaphignathus*; *v.*: *velifer*; *r.*: *rugosa*; *Ps.*: *Pseudopolygnathus*; *Po.*: *Polygnathus; Bi.*: *Bispathodus.*

LAURUSSIA

FAMENNIAN -360Ma

PALEOTETHYS OCEAN

0°

Baltica

Franconia

Bohemia

BU

Saxo Thuringia

Armorica

CT

Corsica-Sardinia

Iberia

30°S

Paleo Adria

RHEIC OCEAN

Amazonia

GONDWANA

Florida

	Continental areas		Marine shelf area		Oceanic area
	Subduction		Fault		

Ziegler & Sandberg (1990)

FAMENNIAN

Pa. expansa — Late, Middle, Early
Pa. postera — Late, Early
Pa. trachytera — Late, Early
Pa. marginifera — Latest, Late, Early
Pa. rhomboidea — Late, Early
Pa. crepida — Latest, Late, Middle, Early
Pa. triangularis — Late, Middle, Early

FRS

Pa. linguiformis
Pa. rhenana

Ma
359.84
362.27
363.01
364.19
366.69
367.73
370.11
372.24
373.04

Buschteich

Col des Tribes

Spalletta et al. (2017)

Bi. ultimus
Bi. costatus
Bi. ac. aculeatus
Pa. gr. expansa
Pa. gracilis manca
Po. styriacus
Ps. granulosus
Pa. r. trachytera
Sc. v. velifer
Pa. marg. utahensis
Pa. marg. marginifera
Pa. gracilis gracilis
Pa. rhomboidea
Pa. gl. pectinata
Pa. glabra prima
Pa. termini
Pa. crepida
Pa. minuta minuta
Pa. del. platys
Pa. triangularis
Pa. subperlobata

-20   0   20   40   60   80 meters

Platform	Slope	Platform	Slope	Platform
Mid ramp	Outer ramp

Sea level

Fair weather wave base

Storm wave base

5

4

3

2

1

Facies 4: Col des Tribes Facies 3

Facies 3: Col des Tribes Facies 2

Facies 2: Buschteich Facies 2 and 3

Facies 1: Col des Tribes Facies 1 and Buschteich Facies 1

Gravitational transportation

Facies 5: Col des Tribes Facies 4

A Axis 1, 77.5%

Axis 2, 18.3%

d = 10

pcBi pcSi pcPa pcSc pcIc pcAn pcPo

B Frasnian

C *Pa. triangularis* to *gl. pectinata*

D *Pa. rhomboidea* to *gr. gracilis*

E *Pa. marg. marginifera* to *Sc. v. velifer*

F *Pa. r. trachytera* to *Ps. granulosus*

G *Po. styriacus* to *Pa. gr. manca*

H *Pa. gr. expansa* to *Bi. costatus*
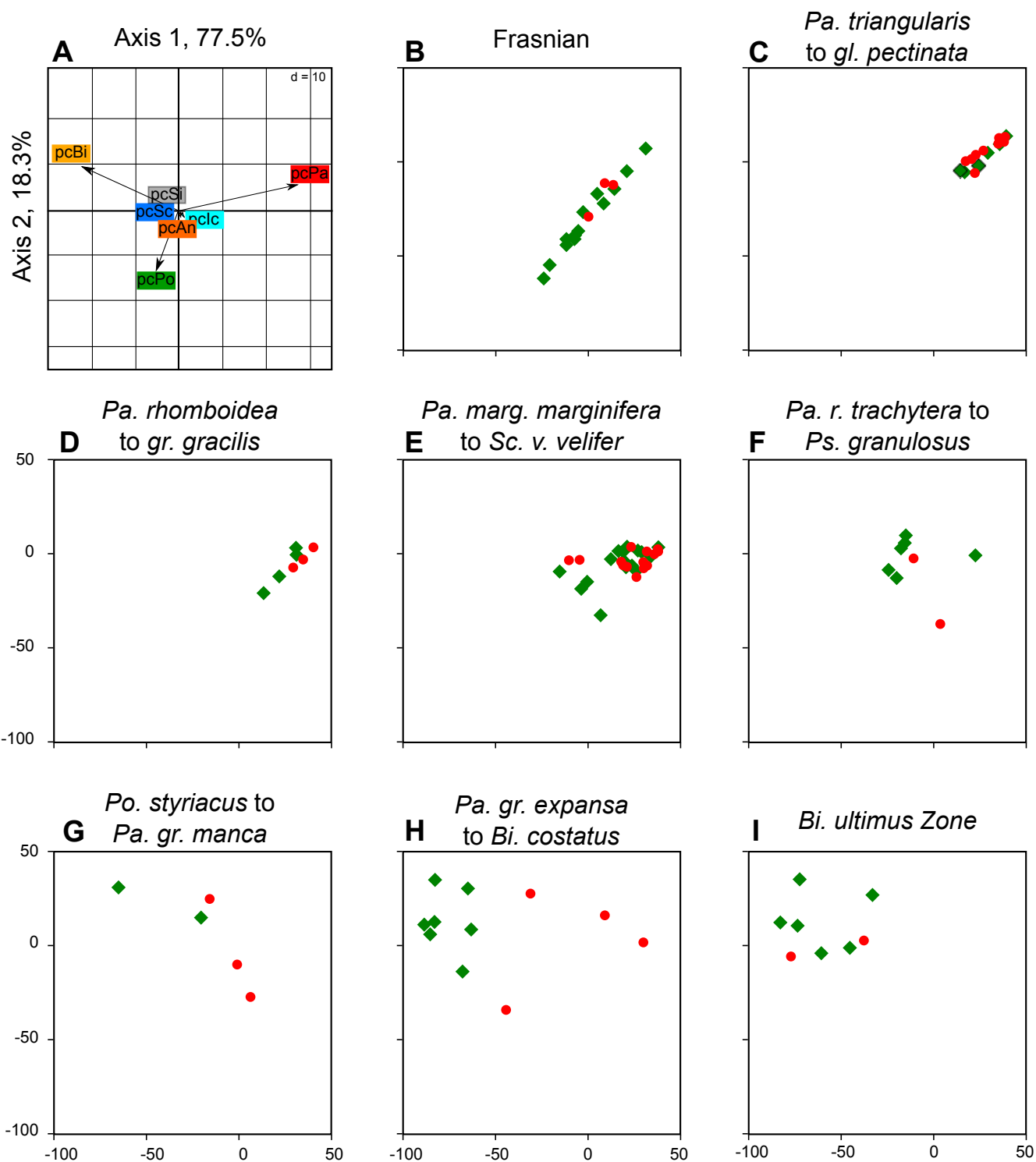
I *Bi. ultimus Zone*

Table 1. Facies and environmental settings for the Col des Tribes and the Buschteich sections

FACIES	DIAGNOSTIC FEATURES	SEDIMENTARY FEATURES	STRATAL PATTERN	BIOCLASTS	DEPOSITIONAL SETTING	Girard et al. *2014 (CT) **2017 (BU)
Facies 1 : pelagic mudstone	Structureless lime mudstone with few bioclasts (2 – 10%)		Well stratified, dms thick	Pelagic ostracods and bivalves, goniatites, radiolarians, rare benthic ostracods, trilobites and crinoids	Outer ramp	Facies 1 at CT and BU
Facies 2: fine-grained turbidites	Laminated wackestone with pelagic fauna and scarce hardparts of benthic organisms	Mm to cm scale thick graded bedding, erosional surfaces at bottom	dm thick beds	Pelagic ostracods and bivalves, radiolarians, some transported benthic ostracods, blind trilobites brachiopods and crinoids	Distal turbidites in outer ramp interbedded within F1	Facies 2 and 3 at BU
Facies 3: pelagic wackestone	Structureless wackestone dominated by pelagic fauna and with 5 % benthic organisms	Pseunodular structure	cm to dm thick beds	Pelagic bivalves and ostracods, diversified cephalopods, radiolarians, crinoids, benthic ostracods and trilobites	Outer ramp, shallower than F1 and F2	Facies 2 at CT
Facies 4: cephalopod wackestone to floatstone (griottes)	Reddish nodular to wavy laminated wackestone to floatstone with abundant goniatites	cm sized lime nodules coated by argillaceous and iron hydroxydes, intraformational breccias, rotated geopetal structures	Cm to dm thick beds	Goniatites, pelagic ostracods and bivalves, trilobites, brachiopods, crinoids and foraminifers	Slope in the upper outer ramp	Facies 3 at CT
Facies 5: wackestone with diversified fauna	Structureless to pseudonodular well stratified wackestone with pelagic and benthic organisms	Pseudonodular structure with cm to dm thick beds	cm to dm thick beds	Pelagic ostracods and abundant goniatites, trilobites, crinoids, brachiopods, gastropods, bivalves, foraminifers	Mid ramp	Facies 4 at CT

Table 2. Relationship between oxygen isotopes, microfacies, and conodont assemblages.

		CT+BU			CT			BU		
		n	R	p	n	R	p	n	R	p
$\delta^{18}O$	Facies	41	0.5023	**0.0008**	22	0.4107	0.0576	19	0.3149	0.1891
Conodont PC1	$\delta^{18}O$	51	-0.5304	**6.2e-5**	25	-0.5665	**0.0031**	26	-0.3039	0.1312
Conodont PC1	Facies	78	-0.6576	**6.1e-11**	52	-0.7058	**5.1e-09**	26	0.1799	0.3791
$\delta^{18}O$	Age	51	-0.5150	**0.0001**	25	-0.7532	**1.388e-05**	26	-0.7018	**6.455e-05**

Correlations between two variables using the Pearson's product-moment correlation, coefficient of correlation (R) and probability (p) are given. Analyses were performed for CT and BU combined, and CT and BU alone. Significant correlations marked in bold (p < 0.05). Age is estimated based on the age model.

Table 3. Analyses of variance on oxygen isotopes and conodont proportions.

	Dependent variable	Independent variable	CT+BU n	Pve	p	CT n	Pve	p	BU n	Pve	p
(1)	$\delta^{18}O$	Age	51	30.5%	**1.83E-09**						
		Section		47.0%	**4.06E-12**						
		Age * Section		0.4%	0.375						
(2)	Conodont PC1	$\delta^{18}O$	41	6.1%	**0.0311**	22	9.0%	**0.0316**	19	11.2%	0.175
		Facies		22.3%	**0.0001**		33.6%	**0.0003**		0.5%	0.769

Two models were considered. (1) A model considered $\delta^{18}O$ as dependent variable, and age, section, and interaction (age * section) as effects. (2) A model considered PC1 based on conodont proportions in the assemblages as the dependent variable. The effects tested were δ $\delta^{18}O$ and facies score. Percentage of variance explained (pve) and probability (p) are given. Significant correlations marked in bold (p < 0.05).